X-ray measurement of the electron static structure factor in LiF

G. Calzuola, C. Petrillo, and F. Sacchetti
Istituto Nazionale per la Fisica della Materia, Unità di Perugia, Perugia, Italy
and Dipartimento di Fisica, Università di Perugia, Via A. Pascoli, I-06123 Perugia, Italy
(Received 7 August 1998)

The x-ray incoherent cross section has been measured in crystalline LiF. The static structure factor and the exchange and correlation energy of valence electrons in LiF have been obtained. Making use of the results of a recent Hartree-Fock calculation in solid LiF, the correlation contribution to the ground-state energy has been determined. The static structure factor data have been analyzed to deduce the valence-electron pair-correlation function. Comparisons have been carried out with the recent quantum Monte Carlo calculations in the homogeneous interacting electron gas. [S0163-1829(99)02620-X]

I. INTRODUCTION

X-ray scattering measurements of the incoherent cross section have been proved to be quite a sensitive tool to investigate electron-electron correlations in light elements.[1–4] By this technique, the electronic static structure factor, which is the Fourier transform of the density-weighted two-body correlation function, can be measured and employed to obtain the exchange-correlation contribution to the ground-state energy of the solid.[5] Extended measurements carried out in beryllium[1] and diamond[2] single crystals have shown that the cohesive energy of the two solids is dominated by the exchange-correlation contribution to the total energy, the deformation of the electron density distribution being a secondary effect.[6] Quite surprisingly, dynamic correlations among valence electrons in both beryllium and diamond were found to be reasonably well described by the interacting electron-gas model at the appropriate densities. Both beryllium, which is a metal, and diamond, which is an insulator, exhibit very similar behaviors as to the static structure factor and hence the pair-correlation function. In both cases, the neutral atomic volume and the absence of charge transfer indicate that the binding is mainly due to the difference between the atom and solid pair-correlation function, the overall shape of the electron-density distribution of the crystals being not remarkably different from that of the free atoms.[6] Based on these findings, a much more systematic study of electron-electron correlations seems to be necessary to clarify the role played by the electron-density distribution either in determining the shape of the Coulomb and Fermi holes surrounding each electron, or in bringing about the binding of the solid.

In order to investigate the relationship between the one-electron density and the pair-correlation function, we carried out a measurement of the incoherent scattering function in LiF by x-ray scattering. The LiF sample was chosen because it has the same average number of electrons per atom as diamond, whereas a strong charge transfer should be present. Therefore, a large contribution to the cohesive energy is expected to be connected with the ionic character of the bonding in this solid. It is also important to note that the average electron density of the noncore electrons in LiF is only slightly smaller than that of diamond, the electron-gas parameter r_s being 1.480 in LiF and 1.317 in diamond. Therefore, information on the exchange-correlation energy functional can be inferred by the comparison of the electron pair-correlation functions in the two systems. The exchange-correlation energy functional is a fundamental quantity for density-functional-based ground-state calculations, and it is routinely approximated by the corresponding quantity calculated for the interacting electron gas.[7–9]

Although LiF is very appealing because of its electron distribution, it is not the best suited material for an experimental study of diffuse scattering since thermal diffuse scattering (TDS) is expected to be quite high due to both the relatively small Li mass and the low Debye temperature.[10] As discussed in previous investigations,[1,2] the only safe way to determine the TDS contribution is through a knowledge of the phonon-dispersion curves as measured by inelastic neutron scattering. Actually, due to the very high neutron absorption cross section of natural lithium, the experimental determination of the phonon dispersion curves in LiF was carried out in a ^{7}Li isotopically substituted LiF crystal,[10] the neutron absorption cross section of ^{7}Li being negligible. Even though strong isotope effects on the phonon-dispersion curves are not expected, some difference could be present. Therefore, the TDS calculation in LiF, which relies on a model dynamical matrix deduced from measured dispersion curves along the maximum symmetry directions, could not be completely reliable, especially at general points in reciprocal space. However, the determination of the TDS by this technique was found to be at an adequate level of accuracy, especially for x-ray scans carried out off the regions close to reciprocal-lattice points.

Recently, a very accurate Hartree-Fock (HF) calculation of solid LiF was performed,[11] and, by means of calculated wave functions, the static structure factor of the solid in the HF limit was obtained.[12] This *exchange-only* calculation, together with the present experimental results, has been extremely useful to point out the contribution of *correlation* effects in LiF. Moreover, since no direction dependence of the static structure factor was observed in the theoretical calculation, the experimental investigation was confined to a limited portion of the reciprocal space.

II. EXPERIMENT AND DATA REDUCTION

The relationship between the measured x-ray differential scattering cross section and the electronic static structure factor was discussed in previous papers.[1,2] Here only the most important steps are reported. The differential cross section for photon scattering off a many-electron system is directly related to the electron density-density correlation function when the photon energy is largely in excess of any absorption edge of the system. In this condition the x-ray cross section is proportional to

$$S(\mathbf{Q}) = S_{ee}(\mathbf{Q}) + S_{TDS}(\mathbf{Q}), \tag{1}$$

where $S_{ee}(\mathbf{Q})$ is the electronic static structure factor, $S_{TDS}(\mathbf{Q})$ is the TDS contribution, and $\mathbf{Q}$ is the momentum transfer. In literature, the quantity $S_{ee}(\mathbf{Q})$ is often referred to as the incoherent scattering factor. Indeed, it is directly related to the energy-integrated Compton scattering cross section which is an incoherent process when the momentum transfer is high enough. Nonetheless, the use of the present notation is aimed at emphasizing the relation between the static structure factor and the pair-correlation function. The experimental data are, of course, affected by additional spurious contributions, like background and multiple scattering, which must be taken into account in the data reduction procedure.

The present experiment was performed using a standard x-ray diffractometer, properly adapted to measure diffuse scattering. In order to minimize the effect of the sample absorption, a rather high incoming photon energy was used, namely, Ag K_α radiation (22.10 keV), resulting in a linear attenuation coefficient $\mu = 1.771\ \mathrm{cm}^{-1}$. The incoming photon energy was much higher than the highest absorption edge in LiF at 0.6768 keV. A pyrolitic graphite monochromator with 0.5° mosaic spread was used to reduce the Bremsstrahlung and to make negligible the K_β contamination of the incoming beam. A 0.5-mm slit was inserted before the monochromator and at 100 mm from the normal-focus tube anode to define the angular divergence of the beam impinging on the monochromator. The beam size at the sample position was $1 \times 10\ \mathrm{mm}^2$, with an angular divergence of 0.6°.

The sample was a slab-shaped single crystal, $1.20 \times 10 \times 10\text{-mm}^3$ dimensions, with all the faces parallel to the (100) crystallographic planes. The transmission coefficient was ~0.75 with the sample, 1.20 mm thick, perpendicular to the beam. Because of the high expected TDS contribution, scans were carried out at different values of temperature. Data collected at the various temperatures were employed to test the reliability of the TDS calculation. The sample was contained into a vacuum chamber having 110-mm diameter and a wide beryllium window, designed to cover a scattering angle range from 0° to 150° in a single scan. The sample was fixed on a copper frame connected to a closed-cycle refrigerator through a heater, so that the temperature could be changed over the range from 20 K to room temperature. The temperature of the sample was measured by means of a Pt resistor fixed on the copper frame with a maximum error of ±0.2 K. During each scan, the temperature was stable within ±0.5 K. To avoid the rotation of the cooling stage or the whole chamber, the scans were performed maintaining the sample in a fixed position, a configuration which allows also for a constant sample volume. A Soller collimator, 100 mm long with Mo blades 1 mm apart, was inserted in between the vacuum chamber and the photon detector. The full aperture of the collimator was $12 \times 12\ \mathrm{mm}^2$, and all the photons scattered within the collimator angular acceptance could be collected at all the scattering angles, the maximum sample size as ''seen'' by this collection system being less than 3 mm. Scattered photons were collected using a standard NaI:Tl scintillator coupled to a photomultiplier, followed by a preamplifier, amplifier, and window discriminator. The x-ray tube was operated at 40 kV, thus avoiding the half-wavelength contamination of the incoming beam.

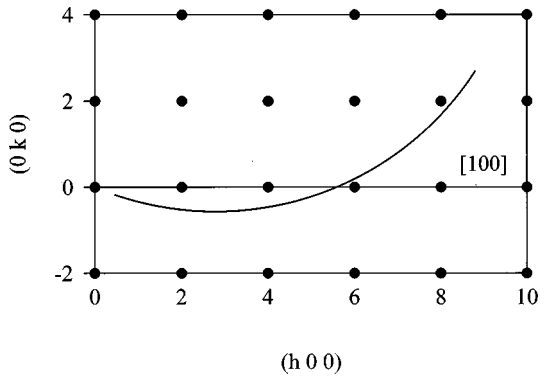

FIG. 1. (001) reciprocal-lattice section of LiF showing the path followed by the $2\dot{\vartheta}$ scan.

The sample was mounted with the [001] crystallographic axis perpendicular to the scattering plane, and its orientation with respect to the incoming beam was determined by rotating it from the actual position to that of the (200) reciprocal-lattice point. In this way the sample position could be determined with an accuracy on the order of the crystal mosaic spread. Although the crystal was of a fairly good quality, with a mosaic spread of the order of 0.1°, some small crystallites were misset by even 1°; therefore the accuracy on the orientation could not be better than ~1°. After some trials, the sample position was selected to end up with the low order reciprocal-lattice points not close to any portion of the scanned region and with the low-angle portion of the scan approximately parallel to the [100] direction. In Fig. 1 the portion of the reciprocal space spanned by the present measurements is shown. As apparent in Fig. 1, the scan direction is rather close to the [100] direction in the region of low momentum transfer, while the high-Q portion of the scan is at general points in the reciprocal space. Based on the HF results of no anisotropy of the static structure factor,[12] the present experimental data can be considered as representative of the [100] direction and of any other direction.

Data were collected at three temperature values, namely 28, 168, and 298 K, with a fixed statistics of 10 000 counts per point. Each scan, extending from 3° to 80°, was repeated ten times. In this way, 100 000 counts per point were collected at all the temperatures, and the statistical error was negligible in comparison with the systematic errors introduced by the various correction steps in the data reduction procedure. The background was measured removing the sample from the copper frame, and collecting the data for the same kind of scans and temperature settings as the sample. It was found to be significant only at low angle where the air

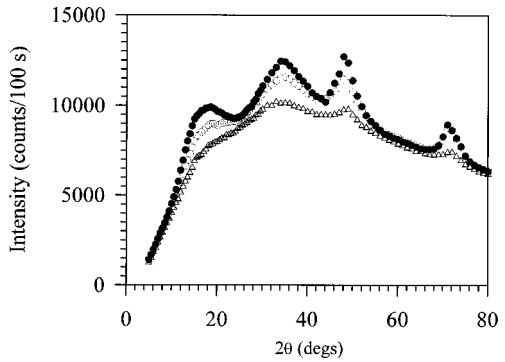

FIG. 2. Measured intensity vs scattering angle after background subtraction [see Eq. (2)]. Dots: $T=298$ K; circles: $T=168$ K; triangles: $T=28$ K.

scattering along the path before the sample chamber was visible by the detector. No temperature dependence of the background was detected. Enough statistics on the background were also accumulated to make the statistical error on the background data negligible in comparison with that of the sample intensity. Finally, the measurement of the background as obtained by substituting the sample with a lead plate was carried out, and an almost zero intensity was found. The background-free intensity of the sample was obtained through the following relationship:

$$I=I_s-T_B(I^0_{\rm back}-I^{\rm Pb}_{\rm back})-I^{\rm Pb}_{\rm back}, \tag{2}$$

where I_s is the intensity measured with the sample in place, $I^0_{\rm back}$ is the background intensity without sample, and $I^{\rm Pb}_{\rm back}$ is the background intensity measured with the lead slab. T_B is the background transmission coefficient[13] along the path from the sample to the detector, and it can be easily calculated once the linear attenuation coefficient μ of the sample is known. The corrected intensity is shown in Fig. 2 at the three temperature values presently investigated.

The electronic static structure factor can be obtained from the measured data after correction for the two unwanted intensity contributions, namely, TDS and multiple scattering. Moreover, the correction for the angle-dependent attenuation must be applied, and a comparison to some reference behavior of the system is necessary to put the corrected intensity on an absolute scale. The correction for the angle-dependent sample attenuation[13] was readily performed in the present case because of the very simple shape of the sample. The same value of the linear attenuation coefficient μ as in the background correction was employed. The multiple-scattering contribution was evaluated by means of a Monte Carlo simulation of the scattering process, following the general treatment presented and discussed in Refs. 13 and 14. The simulation program requires the total and the scattering cross sections of the sample as input data, the latter unknown. Tabulated values[15] of the total cross sections of Li and F were employed, while the scattering cross sections were calculated from the free atom scattering factors and static structure factors,[15] and used as reference input to the program. Multiple scattering was calculated, taking into account all the possible double-scattering processes, including polarization effects, while the total multiple scattering was deduced according to Ref. 13 under the assumption:

$$I_m(k)/I_m(k-1)=I_m(2)/I_1,$$

$I_m(k)$ being the multiple-scattering intensity of order k, and I_1 the single-scattering intensity. The multiple-scattering contribution turned out to be almost isotropic, and of the order of 5% of the average intensity. Considering the low contribution of the multiple scattering, the above assumption on higher-order scattering terms was considered quite adequate.

The TDS contribution was calculated employing the dynamical matrix as deduced from the measured phonon-dispersion relation[10] in ^{7}LiF. Phonon frequencies and eigenvectors at any point of the Brillouin zone were obtained by diagonalization of the dynamical matrix. The one-phonon contribution to TDS was then exactly obtained within the harmonic approximation. Multiphonon contributions were obtained under the quasi-isotropic approximation[16] and using the Debye-Waller factors of Li and F as deduced from the same dynamical matrix. The total TDS contribution turned out to be quite structured and strongly temperature dependent, as expected from the Debye temperature of LiF. The subtraction of the calculated multiple scattering and TDS contributions could be applied to the experimental intensity once on an absolute scale.

The experimental intensity, after background correction, was normalized to the sum of the free-atom theoretical structure factor, TDS, and multiple-scattering contributions at high momentum transfer. This normalization procedure is expected to be quite accurate since at high momentum transfer the static structure factor *must* converge to the number of electrons, and solid-state effects are minimized in this region. To our knowledge, the best available free-atom static structure factor $S_{\rm at}(Q)$ is that deduced from the correlated wave functions obtained from configuration-interaction (CI) calculations. CI calculations of $S_{\rm at}(Q)$ are available for Li but not for F. To carry out the data reduction, $S_{\rm at}(Q)$ of fluorine was deduced by interpolation from the free-atom static structure factors calculated using the CI method in Li,[17] Be,[17] C,[18] and Ne.[19] The reliability of $S_{\rm at}(Q)$ thus obtained for fluorine was checked by calculating the correlation energy term. Indeed, the exchange-correlation energy per atom of a many-electron system is simply related to the static structure factor $S(\mathbf{Q})$ through the following relationship:[5,6]

$$E_{\rm xc}=\frac{e^2}{8\pi^2}\int d\mathbf{Q}\,\frac{S(\mathbf{Q})-Z}{Q^2}. \tag{3}$$

Inserting the structure factor calculated from HF wave functions into Eq. (3), the exchange-only energy contribution is obtained. The correlation energy term, associated with a given $S(\mathbf{Q})$, is given by the difference between the corresponding exchange-correlation energy and the exchange-only HF energy. Actually, the correlation energy contains also the scattering factor contribution arising from the difference between CI and HF wave functions. However, this last contribution is rather small,[17,18] being less than 10% in Li, Be and Ne. Applying this procedure to the fluorine-free atom, with the HF calculation of $S_{\rm at}(Q)$ from Ref. 15, a correlation energy of -0.56 Ry was obtained from the interpolated CI free-atom static structure factor of fluorine. Such a value should be compared with the best estimate of correlation energy available for F, that is, -0.650 Ry.[20] There-

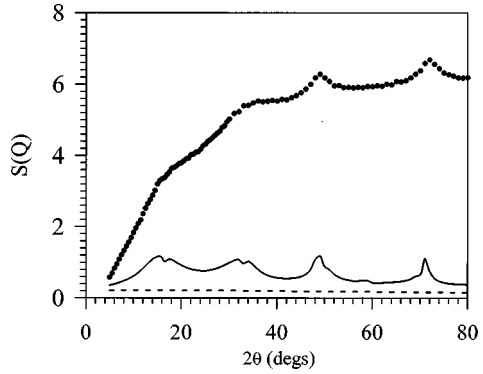

FIG. 3. Measured static structure factor $S(Q)$ [Eq. (1)] vs scattering angle. The calculated TDS contribution $S_{\mathrm{TDS}}(Q)$ (full line) and the multiple-scattering contribution (dashed line) are shown (see text).

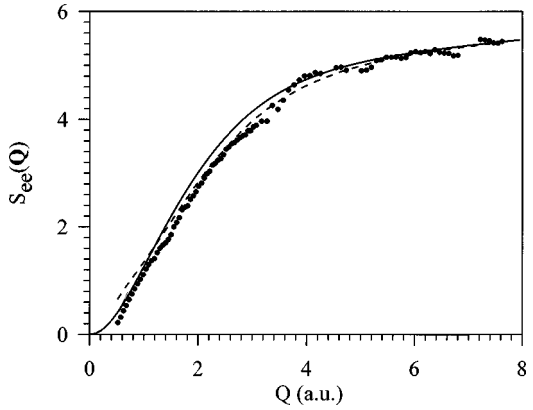

FIG. 4. Measured static structure factor $S_{\mathrm{ee}}(\mathbf{Q})$ vs momentum transfer. The calculated free-atom static structure factors are also shown (see text). Dashed line: CI free-atom calculation. Full line: HF free-atom calculation.

fore, a substantial fraction of the correlation energy is accounted for by the interpolated static structure factor which was assumed as a good estimate for the free fluorine atom. Making use of $S_{\mathrm{at}}(Q)$ of Li and F, the scale factor for the experimental data normalization from 50° to 80° was determined and TDS, and multiple-scattering contributions were subtracted.

Finally, the data were corrected for polarization effects, by assuming an unpolarized incoming photon beam, as obtained by previous measurements of the linear polarization on the same experimental apparatus,[1,2] and resulting from the low takeoff angle at the graphite monochromator. The kinematic factor was also taken into account according to the procedure described in the case of diamond.[2] In Fig. 3 the normalized data at 28 K are shown in comparison with TDS and multiple-scattering contributions. The data were normalized to 6, the average number of electrons per atom. An inspection of Fig. 3 shows that the TDS contribution is still quite appreciable at this low temperature, and that the calculated TDS curve accounts fairly well for the complex features observed in the experimental data. Nonetheless, it is also evident that in the region where the TDS is large the calculated data fail to account precisely for the most prominent features of the experimental data. This effect is even more pronounced at higher temperatures, thus indicating that the dynamical matrix of Ref. 10 is adequate to describe the phonon-dispersion curves, but use of the harmonic approximation contains some failure. In any case, by an internal comparison of the experimental results at the three temperatures, it was possible to give an estimate of the rms error on the static structure factor normalized as in Fig. 3, which turned out to be of the order of 0.05 electron units. Finally, the data from regions close to the TDS maxima were removed and the final results are shown in Fig. 4, where the electron-electron static structure factor $S_{\mathrm{ee}}(\mathbf{Q})$, as obtained from the present data at the lowest temperature, is compared with the free atom $S_{\mathrm{at}}(Q)$ obtained from both CI and HF results. The agreement between the experimental data and both atomic calculations is very good at momentum-transfer values higher than 4 a.u., thus confirming the reliability of the present normalization procedure.

III. DATA ANALYSIS AND CONCLUSION

From the static structure factor data of crystalline LiF shown in Fig. 4, information about the electron-electron correlations in this system can be obtained. First of all, the exchange-correlation energy of the crystal, which is simply related to $S_{\mathrm{ee}}(\mathbf{Q})$ through Eq. (3), was deduced and found to be $E_{\mathrm{xc}}=-6.39\pm0.04$ Ry/atom. The exchange-correlation contribution to the cohesive energy of the crystal was obtained by taking the difference with the exchange-correlation energy of the free atom calculated with the CI $S_{\mathrm{at}}(Q)$ through Eq. (3). It resulted to be $E_{\mathrm{xc}}^{\mathrm{coh}}=0.15\pm0.04$ Ry/atom. Since the total cohesive energy of LiF, with respect to the free neutral atoms, from thermochemical measurements is 0.32 Ry/atom, the exchange-correlation contribution to the LiF cohesion is about 50%. This behavior is different from that observed in beryllium[6] and diamond,[2] where the cohesion was dominated by the exchange-correlation contribution. In LiF the cohesion is largely contributed by the Coulomb energy, that is, the Hartree electrostatic term plus the electron-nucleus interaction. The deformation of the electron density, occurring in solid LiF with respect to the neutral free atoms, has a role in LiF cohesion. This behavior should be connected to the ionic nature of the bonding in LiF, thus explaining why the simple traditional approach to the cohesion in ionic crystals gives a fairly good estimate of the cohesive energy. In beryllium and diamond the electron-density deformation is much smaller, as shown by the close overall similarity of the scattering factors in the solid and atomic phases, although solid-state effects play a role specially in diamond.

The correlation energy term can be obtained making use of the recent Hartree-Fock calculation of the static structure factor of solid LiF.[12] As in the case of the free atom, assuming that the HF calculation produces a good one-electron density, the correlation energy is given by the difference between the true exchange-correlation energy and that calculated using the HF wave functions. From the present experimental data, after subtraction of the HF result,[12] a correlation energy of -0.56 ± 0.04 Ry/atom was deduced for solid LiF. Such a value has to be compared with the correlation energy of the free Li and F atoms obtained by applying the same procedure. The free-atom correlation energy, equal to one-half of the sum of Li and F correlation energies, was found to be -0.33 Ry/atom. These results show that the correlation energy in solid LiF is higher than that of the free atoms by an

amount comparable with the exchange-correlation contribution to the cohesive energy. Therefore, correlation effects should not be neglected in this ionic solid and, perhaps, in other ionic systems.

It is interesting to observe that the experimental structure factor $S_{ee}(\mathbf{Q})$ of solid LiF is not very well reproduced by the simple superposition of Li and F free-atom structure factors. Although the low value of E_{xc}^{coh} is brought about by the overall small difference $[S_{ee}(\mathbf{Q})-S_{at}(Q)]$, systematic differences between solid and free atoms are detected. The experimental data can be further analyzed in order to extract real-space information about the electron-electron correlations in the solid. In principle, the static structure factor $S_{ee}(\mathbf{Q})$ is directly related to a proper average of the two-body correlation function[2] through

$$\overline{g}(\mathbf{r})=\frac{1}{(2\pi)^3\overline{n}Z}\int d\mathbf{Q}[S_{ee}(\mathbf{Q})-Z]e^{i\mathbf{Q}\cdot\mathbf{r}}, \tag{4}$$

where the position-averaged pair-correlation function $\overline{g}(\mathbf{r})$ is a measure of the probability of finding two electrons at a distance $\mathbf{r}$ independently of their individual positions relative to the crystal, and $\overline{n}$ is the average number density. However, such a relationship is of little use as the long-range part of $S_{ee}(\mathbf{Q})$ must be accurately known to carry out the integration. Because of the very slow asymptotic trend of $S_{ee}(\mathbf{Q})$ as Q diverges,[21] $\overline{g}(r)$ can be hardly determined by a direct Fourier analysis.

The study of the pair-correlation function was carried out by splitting the experimental static structure factor into three contributions:

$$S_{ee}(\mathbf{Q})=S_{core}(\mathbf{Q})+S_{val}(\mathbf{Q})+S_{int}(\mathbf{Q}), \tag{5}$$

where $S_{core}(\mathbf{Q})$, $S_{val}(\mathbf{Q})$, and $S_{int}(\mathbf{Q})$ refer to core-core, valence-valence, and valence-core correlations. Actually, Eq. (5) is meaningful only in the one-electron approximation, where the one-electron wave functions are well defined and the associated energy eigenvalues can be identified as core or valence states. Nonetheless, considering that the one-electron energy spectrum shows a well-defined energy separation, $S_{val}(\mathbf{Q})$ can be obtained from the experimental $S_{ee}(\mathbf{Q})$ under suitable approximations for $S_{core}(\mathbf{Q})$ and $S_{int}(\mathbf{Q})$. Following the procedure described in Refs. 1 and 2, $S_{core}(\mathbf{Q})$ was described by the CI calculations for free ions by Thakkar and Smith,[22] while $S_{int}(\mathbf{Q})$ was modeled by the HF calculation of solid LiF by Shukla.[12] The latter contribution was almost negligible in beryllium and diamond, but it turned out to be appreciable in LiF, being of the order of 0.1 electron units. The static structure factor $S_{val}(\mathbf{Q})$, thus deduced, was employed to study the real-space behavior of the pair-correlation function of the valence electrons. In the case of beryllium and diamond, a model pair-correlation function for the interacting electron gas was employed and the analytical Fourier inversion of this model function was compared with the experimental data. Direct application of this approach to LiF is prevented by the remarkable electron-density difference expected at the Li and F sites. To take into account the electron-density inhomogeneity of the present system, the experimental valence static structure factor was fitted to the equation:

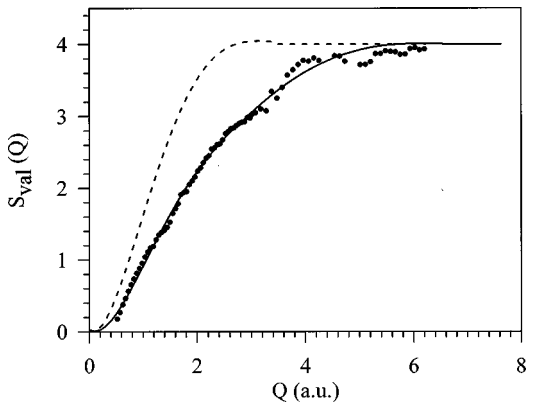

FIG. 5. Experimental valence static structure factor $S_{val}(\mathbf{Q})$ [Eq. (5)] vs momentum transfer. Full line: fit to the experimental data according to Eq. (6). Dashed line: quantum Monte Carlo results (Ref. 23) for the homogeneous interacting electron gas at $r_s=1.480$.

$$S_{val}(\mathbf{Q})=Z_1S_h(Q,n_1)+Z_2S_h(Q,n_2), \tag{6}$$

where $S_h(Q,n)$ is the static structure factor of the homogeneous interacting electron gas with density n. The fit was carried out employing the $S_h(Q,n)$ electron-gas data obtained by the quantum Monte Carlo simulation of Ortiz and Ballone,[23] and leaving n_1, n_2, Z_1, and Z_2 as free parameters with the additional condition $Z_1+Z_2=4$. The results of this procedure are shown in Fig. 5. It is apparent that the model of Eq. (6) accounts extremely well for the experimental $S_{val}(\mathbf{Q})$, apart from the region where the subtraction of $S_{TDS}(\mathbf{Q})$ is less satisfactory, the rms error being less than 0.02 electron units over the whole range. From the fit of Eq. (6), the following average pair correlation function can be readily obtained:

$$\overline{g}(r)=\frac{1}{Z_1n_1+Z_2n_2}[Z_1n_1g_h(r,n_1)+Z_2n_2g_h(r,n_2)], \tag{7}$$

where

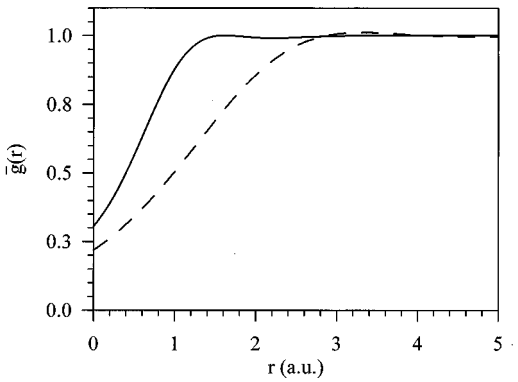

FIG. 6. Valence pair correlation function in LiF. Full line: curve obtained by analytic Fourier inversion of the static structure factor fitted to the experimental data according to Eq. (6) (see text). Dashed line: quantum Monte Carlo results (Ref. 23) for the homogeneous interacting electron gas at $r_s=1.480$.

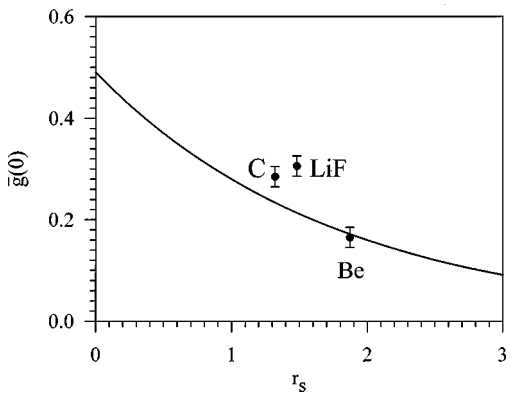

FIG. 7. Zero-separation pair correlation function versus r_s. Dots: experimental data in beryllium (Ref. 1), diamond (Ref. 2), and LiF. The full line is the quantum Monte Carlo curve for the homogeneous interacting electron gas from Ref. 23.

$$g_h(r,n)=1+\frac{1}{2\pi^2 nr}\int_0^\infty dQ[S_h(Q,n)-1]Q\sin(Qr) \tag{8}$$

is the pair-correlation function of the electron gas with density n, as reported in Ref. 23. The resulting pair-correlation function $\overline{g}(r)$ is presented in Fig. 6 in comparison with that appropriate to a homogeneous interacting electron gas having the same average valence density as LiF. As both Figs. 5 and 6 show, the homogeneous interacting electron-gas model remarkably fails in reproducing the experimental data in both Q and r spaces, whereas the model of Eq. (6) is quite adequate, thus suggesting that the pair-correlation function is defined by the local density. In fact, Eq. (6) and the results of the fit state that a proper average density at Li and F sites is the relevant parameter which can be used to describe the electron-electron correlations in LiF. The best fit parameters were found to be: $Z_1=0.91\pm0.02$, $r_{s_1}=1.8\pm0.2$, $Z_2=3.09\pm0.02$, and $r_{s_2}=0.708\pm0.010$, and clearly indicate that a small number of low-density electrons together with a higher number of high-density electrons are necessary to describe the correlation function of LiF. This behavior is an experimental evidence of the local-density approximation[7] often employed in the theoretical description of electron states in real solids.

A further comparison with the electron-gas results can be carried out by making use of the zero-separation pair-correlation function data in beryllium,[1] diamond,[2] and LiF. These data are shown in Fig. 7 in comparison with the quantum Monte Carlo curve of $g_h(0)$ versus r_s from Ref. 23. The $\overline{g}(0)$ value found in LiF cannot be accounted for by the expected density dependence of the homogeneous interacting electron gas. This behavior is a clear consequence of the inhomogeneity of the electron density in the unit cell of this system. Indeed, from Eq. (7) the zero-separation pair-correlation function is a weighted average of the two components and, because of the density dependence of $g_h(0)$, it is dominated by the regions where the density is higher, and it receives high values. The same trend is observed when the homogeneous interacting electron gas parameter

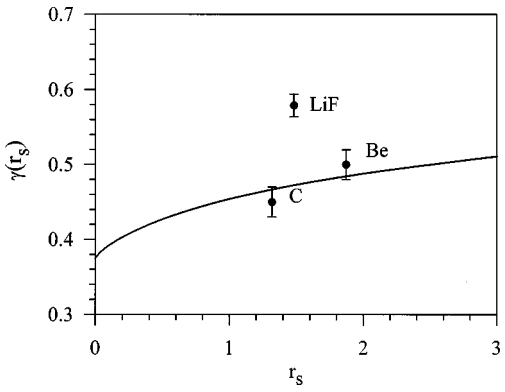

FIG. 8. γ parameter vs r_s (see text). Dots: experimental data in beryllium (Ref. 1), diamond (Ref. 2), and LiF. The full line is the theoretical quantum Monte Carlo result for the homogeneous interacting electron gas from Ref. 24.

$$\gamma=\frac{1}{2k_F}\int_0^\infty dQ[1-S_h(Q)] \tag{9}$$

is compared with the appropriate γ values deduced from the experimental data in beryllium, diamond, and LiF. In the homogeneous electron gas, the γ parameter is directly related to the correlation energy, while in the inhomogeneous electron system it is related to the ground-state exchange-correlation energy through Eq. (3). Using the present static structure factor data and k_F as deduced from the average electron density, the value $\gamma=0.579\pm0.005$ was found. In Fig. 8 the γ values obtained in beryllium, diamond, and LiF are shown in comparison with the electron-gas data. Again, LiF behaves quite differently from the other two systems, the experimental γ parameter being a weighted average of different values.

As a conclusion, we can say that, contrary to the previous findings in the pure elements beryllium and diamond, strong effects brought about by the one-electron density inhomogeneity are present in LiF, and these effects show up as the evident departure of the valence-electron static structure factor from that of the homogeneous interacting electron gas at the average density. Moreover only a 50% contribution to the cohesive energy from the exchange-correlation term was found, the remaining 50% of the cohesive energy being due to the one-electron density deformation. Thanks to the availability of a Hartree-Fock calculation[12] of the static structure factor in solid LiF, the correlation energy contribution was determined and found to be higher than that of the free atoms. Finally, the present findings suggest that systematic calculations of the HF static structure factors in light elements, coupled to experimental investigations in materials other than Be, C, and LiF, could help in understanding the role of the electron-electron correlations in solid cohesion.

[1] G. Mazzone, F. Sacchetti, and V. Contini, Phys. Rev. B **28**, 1772 (1983).
[2] C. Petrillo and F. Sacchetti, Phys. Rev. B **51**, 4755 (1995).
[3] C. B. Walker, Phys. Rev. **103**, 558 (1956).
[4] T. Paakkari and P. Suortti, Phys. Rev. B **9**, 1756 (1974).
[5] G. Mazzone and F. Sacchetti, Phys. Rev. B **30**, 1739 (1984).
[6] C. Petrillo, F. Sacchetti, and G. Mazzone, Acta Crystallogr., Sect. A: Found. Crystallogr. **54**, 468 (1998).
[7] R. O. Jones and O. Gunnarsson, Rev. Mod. Phys. **61**, 689 (1989).
[8] J. P. Perdew, J. A. Chevary, S. H. Vosko, K. A. Jackson, M. R. Pederson, D. J. Singh, and C. Fiolhais, Phys. Rev. B **46**, 6671 (1992).
[9] G. D. Mahan, *Many-Particle Physics* (Plenum, New York, 1991), Chap. 5.
[10] G. Dolling, H. G. Smith, R. M. Nicklow, P. R. Vijayaraghavan, and M. K. Wilkinson, Phys. Rev. **168**, 970 (1968).
[11] A. Shukla, M. Dolg, P. Fulde, and H. Soll, Phys. Rev. B **57**, 1471 (1998).
[12] A. Shukla (unpublished).
[13] C. Petrillo and F. Sacchetti, Acta Crystallogr., Sect. A: Found. Crystallogr. **46**, 440 (1990).
[14] C. Petrillo and F. Sacchetti, Acta Crystallogr., Sect. A: Found. Crystallogr. **48**, 508 (1992).
[15] *International Tables for X-ray Crystallography* (Kynoch, Birmingham, 1989), Vol. IV.
[16] J. E. Eldridge and T. R. Lomer, Proc. Phys. Soc. London **91**, 459 (1967).
[17] R. T. Brown, Phys. Rev. A **2**, 614 (1970).
[18] R. T. Brown, Phys. Rev. A **5**, 2141 (1972).
[19] E. M. Peixoto, C. F. Bunge, and R. A. Bonham, Phys. Rev. **181**, 322 (1969).
[20] S. J. Chakravorty, S. R. Gwaltney, E. R. Davidson, F. A. Parpia, and C. F. Fischer, Phys. Rev. A **47**, 3649 (1993).
[21] A. Rajagopal, J. C. Kimball, and M. Banerjee, Phys. Rev. B **18**, 2339 (1978).
[22] A. J. Thakkar and V. H. Smith, J. Phys. B **11**, 3803 (1978).
[23] G. Ortiz and P. Ballone, Phys. Rev. B **50**, 1391 (1994).
[24] D. M. Ceperley and B. J. Alder, Phys. Rev. Lett. **45**, 566 (1980).